*Desalination and Water Treatment*
www.deswater.com

doi: 10.1080/19443994.2013.822158

52 (2014) 6464–6473
October

Taylor & Francis
Taylor & Francis Group

# Removal and recovery of Cr (VI) by magnetite nanoparticles

M.R. Lasheen[a], I.Y. El-Sherif[a], Dina Y. Sabry[b], S.T. El-Wakeel[a,*], M.F. El-Shahat[b]

[a]*Water Pollution Research Department, National Research Centre, 12311, Dokki, Cairo, Egypt*
*Tel. +202 33370931; Fax: +202 33371211; email: shaimaa_tw@yahoo.com*
[b]*Faculty of Science, Ain Shams University, Cairo, Egypt*

Received 3 September 2012; Accepted 17 June 2013

ABSTRACT

The removal efficiency of Cr (VI) from aqueous solutions using magnetite nanoparticles was investigated. Structural characterization of the nanoparticles prepared by the coprecipitation method showed that an average particle size of 2 and 7 nm confirmed by transmission electron microscopy image. The surface area was determined to be 125 $m^2/g$ using Brunauer-Emmet-Teller method. Batch experiments were carried out to determine the adsorption equilibrium of Cr (VI) by these magnetite nanoparticles as a function of contact time, pH, initial metal concentration, and adsorbent dose. Adsorption equilibrium was reached within 30 min and independent of initial Cr (VI) concentration. The adsorption process was found to be pH dependent and fits well with the Langmuir and Freundlich isotherm equations. Kinetics of the adsorption followed the pseudo-second-order model.

*Keywords:* Magnetite; Nanoparticles; Chromium; Adsorption; Recovery

## 1. Introduction

Toxic heavy metals contamination is a serious problem threatening human health [1,2]. They are not biodegradable and can accumulate in living organisms [3].

Chromium has been put on the top priority list of toxic pollutants by the US Environmental Protection Agency (USEPA) and is present in aqueous systems in both the trivalent form and the hexavalent form. The major hexavalent chromium pollution sources are directly related to the industrial activities including electroplating, steel, and textile industries as well as cooling towers, tanning, and oxidative dyeing industries with hexavalent chromium being transferred to the environments through wastewater release [4].

The USEPA recommends that the levels of chromium in water should be reduced to 0.1 mg/L to protect against skin reactions known as "allergic dermatitis" [5,6].

Studies in both animals and people show that exposure to hexavalent chromium via drinking water leads to elevated chromium levels in tissues, particularly the gastrointestinal tract, blood, liver, kidneys, and spleen, and in increased toxicity [7,8]. The EPA's new analysis of hexavalent chromium toxicity, in 2010, cites significant cancer concerns linked to exposure to the contaminant in drinking water. It highlights the health effects documented in animal studies, including anemia and damage to the gastrointestinal tract, lymph nodes, and liver.

In response to this study and others, California officials in the USA last year proposed setting a public health goal for chromium (VI) in drinking water of

*Corresponding author.

0.06 ppb. This is the first step toward establishing a statewide enforceable limit [9].

Several technologies including chemical precipitation, ion exchange, reverse osmosis, adsorption, etc. have been used to remove heavy metal ions from various aqueous solutions [10,11]. Among these methods, adsorption has increasingly received much attention in recent years because the method is simple, relatively low-cost, and effective in removing heavy metal ions from water and wastewater, especially at low metal ion concentrations [12].

Many kinds of adsorbents for treatment have been developed, such as activated carbon [13], activated alumina [14], coated silica gel [15], and treated sawdust [16]. Recently, there has been growing interest in using adsorption materials with large specific external surface area, easy recycling, and high reusability [10–16].

With the rapid development of nanotechnology, nanoparticles are currently studying widely. Nanoadsorbents found to have particularly high adsorption capacities for metal ions removal from aqueous solutions because of their specific functionality, extremely small size, large specific surface areas, and high reusability.

Magnetic separation has been shown to be a very promising method for solid–liquid phase separation technique [17]. Superparamagnetic iron oxide ($Fe_3O_4$) nanoparticles have been applied in various fields such as physics, medicine, biology, environmental applications, and materials science due to their small size and superparamagnetism so that they can be easily recovered with an external magnetic field and have low toxicity [18].

Magnetite nanoparticles in this study prepared by the coprecipitation method and characterized by transmission electron microscopy (TEM), X-ray diffraction (XRD), and Brunauer-Emmet-Teller (BET).

The objectives of this study are to (1) Assess the prepared magnetite nanoparticles for removing Cr (VI) from aqueous solutions. (2) Investigate the effect of experimental conditions (e.g. pH value, contact time, adsorbent dose, and initial Cr (VI) concentration) on chromium removal. (3) Study the adsorption isotherm, equilibria, and kinetics of Cr (VI) adsorption onto the prepared magnetite nanoparticles.

Also, the reusability of prepared nanomagnetite and Cr (VI) desorption after several recycling periods were checked to show the efficiency of the separation process.

The study provides potential application of nanomagnetite for Cr (VI) adsorption from industrial wastewater even at very low concentrations. Another important advantage of using nanomagnetite for the removal of environmental pollutants lie in the fact that they cost-effectively meet the environmental regulations for wastewater treatment.

## 2. Experimental

### 2.1. Synthesis of magnetite nanoparticles

Magnetite nanoparticles were prepared via improved chemical coprecipitation method [19,20]. A 2:1 M ratio of $Fe^{2+}$ and $Fe^{3+}$ ions was dissolved in deionized water using anhydrous ferric chloride $FeCl_3$ and ferrous chloride tetrahydrate $FeCl_2.4H_2O$.

Chemical precipitation was achieved by adding $NH_4OH$ solution (25%) till the final pH attained to 10–12 with maintaining vigorous stirring for 2 h. The precipitates were heated to 80 °C for 30 min, and then washed three times with distilled water and one time with anhydrous ethanol. The particles were then dried in an oven at 70 °C.

### 2.2. Characterization of adsorbent

The structural characterization of the prepared magnetite nanoparticles was conducted by powder X-ray diffraction spectrometry using Bruker D8 advance instrument. The instrument was equipped with a copper anode generating (Cu-K$\alpha$) radiation ($\lambda$ = 1.5406 Å).

TEM for size investigation and morphology identified using JOEL JEM (1230) electron microscope instrument with resolving resolution of 0.2 nm.

Gas adsorption analyzer with BET method (Quantachrome NOVA Automated gas sorption system sorb-1.12) was used for the surface area determination. The method was carried out under relatively high vacuum, where $N_2$ gas was used as adsorbate at 77 K.

Point zero charge (PHpzc) for the adsorbent was determined, 0.01 M NaCl was prepared, and its pH was adjusted in the range of 2–12 by adding NaOH or HCl. About 50 mL of 0.01 M NaCl was put in a number of conical flasks and then 0.25 g of the adsorbent was added to the solution at the different pH values [21]. The flasks were kept for 48 h and the final pH of the solution was measured. Graphs were then plotted for pH final vs. pH initial.

The concentration of Cr (VI) in the solution was determined according to APHA (2005) [22] using atomic absorption spectrometer (Varian Spectra AAS 220) with graphite furnace accessory and equipped with deuterium arc background corrector. The precision of the metal measurement was determined by analyzing (in triplicate) the metal concentration of all

samples, and for each series of measurements an absorption calibration curve was constructed.

### 2.3. Adsorption studies

The adsorption behavior of the prepared magnetite nanoparticles for Cr (VI) was investigated by means of the batch experiments at room temperature. A known amount of magnetite nanoparticles was mixed with Cr (VI) solution over a period of time on a shaker at 200 rpm. All the experiments were carried out in triplicate and the mean of the quantitative results were used for further calculations. After that, the aqueous phase was separated by magnetic decantation followed by filtration.

The adsorption of Cr (VI) by prepared magnetite nanoparticles for Cr (VI) was investigated in the pH range of 2–9. The solution pH was adjusted by 0.1 M NaOH or 0.1 M $HNO_3$. The effects of contact time (10–140 min), initial Cr (VI) concentration (5, 20, 50, and 100 mg/L), and amounts of adsorbent dosage (0.1–4 g/L) were also examined throughout the experiments at room temperature.

The equilibrium adsorption capacity, $q_e$ (mg/g), of Cr (VI) aqueous was calculated using the mass balance, according to the following equation:

$$q_e = \frac{C_o - C_e}{M} XV \quad (1)$$

where $V$ is the sample volume (L), $m$ is the mass of the adsorbents (g), $C_o$ is the initial concentration of Cr (VI) (mg/L), and $C_e$ is the equilibrium concentration of Cr (VI) in the solution (mg/L).

### 2.4. Sorption isotherms

Adsorption isotherm studies were conducted by varying the initial Cr (VI) concentration from 100 to 400 mg/L using different sorption models.

### 2.5. Sorption kinetics

The kinetics of the sorption process describe the solute uptake and provides useful data regarding the efficiency of the adsorption and the feasibility for scale-up operations. Different models were used to analyze the kinetics of the sorption process.

### 2.6. Desorption of Cr (VI) and reusability of nano magnetite

Desorption of Cr (VI) from Cr-loaded nanoadsorbent was performed using two different eluents, $HNO_3$ and HCl solutions, at different concentrations (1 and 5 M). The mixture was agitated at 200 rpm for 2 h.

After desorption, the nanoadsorbent was separated by a small magnet followed by filtration and Cr (VI) concentration measured. The recovery efficiency, $r$ (%), of Cr (VI) from the solid phase was calculated as follows [23]:

$$r(\%) = \frac{C_{des}}{C_{ads}} \times 100 \quad (2)$$

where $C_{des}$ and $C_{ads}$ are the amount of Cr (VI) released into the aqueous solution and the amount of Cr (VI) adsorbed onto the magnetite nanoadsorbents (mg/L), respectively.

To test the reusability of the nanoadsorbent, 10 mL of 100 mg/L Cr (VI) solution was adsorbed by 20 mg of Cr (VI)-loaded nanomagnetite for 2 h and then desorbed with the addition of 10 mL of 5 M $HNO_3$ and stirring for 2 h. After each cycle of adsorption–desorption, the adsorbent was washed thoroughly with distilled water to neutrality, then dried, and reconditioned for adsorption in the succeeding cycle.

## 3. Results and discussion

### 3.1. Characterization of magnetite nanoparticles

The TEM image for magnetite nanoparticles is shown in Fig. 1. Most magnetite nanoparticles exhibit spherical shape and have a particle size range from 2 to 7 nm. The BET surface area of magnetite nanoparticles was 125 $m^2/g$.

The XRD pattern of the prepared magnetite nanoparticles compared with JCPDS reference pattern of magnetite (No. 19-0629) are shown in Fig. 2.

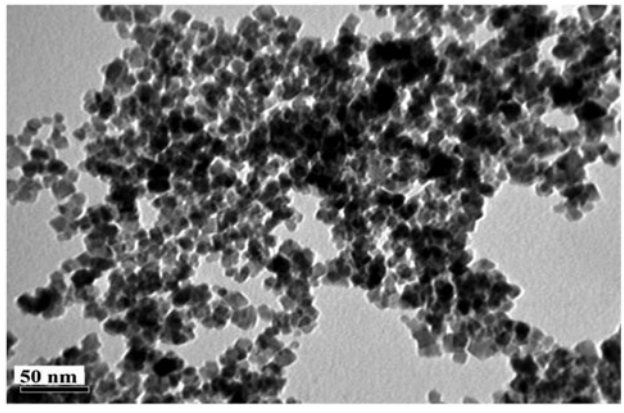


Fig. 1. TEM images of magnetite nanoparticles.

Six characteristic peaks for magnetite ($2\theta = 30.1$, 35.5, 43.1, 53.4, 57.0, and 62.6°) and the position (35.5°) of the most intense line in the XRD pattern are shown. No peak of the other component except magnetite has been detected in this sample. The XRD patterns of the prepared magnetite nanoparticles matched well with JCPDS reference pattern (No. 19-0629) of magnetite [24] (Fig. 3.)

pHpzc was determined for magnetite nanoparticles adsorbent. PHpzc indicates the electrical neutrality of the adsorbent and surface at a particular value of pH. The graph of pH initial vs. pH final was plotted. The intersection of the curve with the straight line is known as the point of the pHpzc, and the value is 6.2.

### 3.2. Adsorption studies

#### 3.2.1. Effect of contact time and initial concentration

The effect of contact time and initial concentration of Cr (VI) on its removal from aqueous solutions was carried out by monitoring its adsorption onto magnetite nanoadsorbent for 140 min. The initial Cr (VI) concentrations were 5, 20, 50, and 100 mg/L, with an adsorbent dose of 2 g/L.

The observed removal rates of Cr (VI) at different initial concentrations are shown in Fig. 4. The removal efficiencies were 88 and 95% for Cr (VI) initial concentrations of 100 and 5 mg/L and equilibrium was achieved within 60 min, independent of the initial concentration of Cr (VI). The conclusion that the removal percentage of Cr (VI) decreased with increasing concentration for a given amount of adsorbent was also obtained by Hu et al. [25].

#### 3.2.2. Effect of pH

It is well known that pH is one of the most important factors which affect the adsorption process. Experiments were performed to find the optimum pH on the adsorption of Cr (VI) onto magnetite nanoadsorbent using different initial pH values changing from 2 to 9. Fig. 4 presents the effects of initial pH on

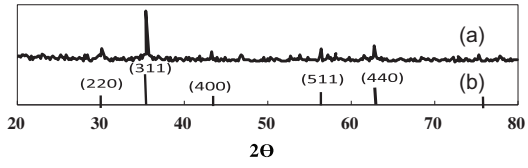


Fig. 2. XRD pattern of (a) Prepared magnetite nanoparticles (b) Magnetite reference database (JCPDS No. 19-0629).

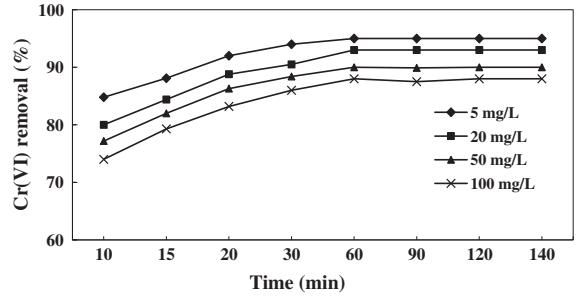


Fig. 3. Effect of contact time and initial concentration on Cr (VI) removal (magnetite dose: 2 gm/L, initial metal concentration: 5, 20, 50, and 100 mg/L, and shaking rate: 200 rpm).

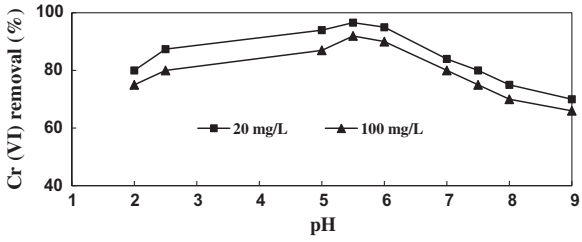


Fig. 4. Effect of initial pH on Cr (VI) removal (magnetite dose: 2 g/L, contact time: 60 min, initial metal concentration: 20, and 100 mg/L, and shaking rate: 200 rpm).

the adsorption of Cr (VI) at initial concentrations 20 and100 mg/L at room temperature and adsorbent dose 2 g/L. Adsorption efficiencies increased gradually from pH 2. The maximum adsorption efficiencies were 96.6 and 88% at pH 5.5 for initial concentrations 20 and 100 mg/L, respectively, then adsorption decreased with increasing pH.

According to Hu et al. [25], Cr (VI) adsorption by magnetite was a combination of electrostatic attraction and ligand exchange at various pH conditions.

#### 3.2.3. Effect of adsorbent dose

Adsorbent dose is an important parameter in the determination of adsorption capacity. As the adsorbent dosage increases, the adsorption sites available for Cr (VI) are also increased and consequently better adsorption takes place. The adsorbent doses were varied from 0.1 to 4 g/L for 5, 20, and 100 mg/L Cr (VI) solutions, while all the other variables such as rpm, contact time, and temperature were kept constant. Fig. 5 revealed that the removal of Cr (VI) increased with increasing magnetite dose. Adsorption reached equilibrium using 2 g/L of adsorbent.

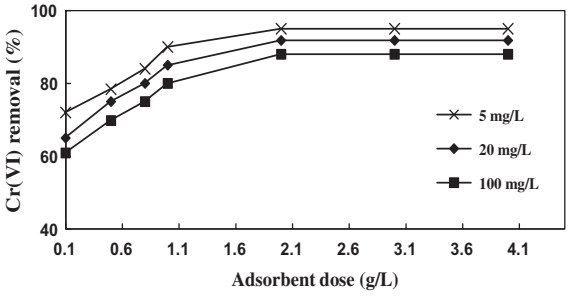


Fig. 5. Effect of adsorbent dose on Cr (VI) removal (magnetite dose: 2 g/L, contact time: 60 min, initial metal concentration: 5, 20, and 100 mg/L, pH: 5.5, and shaking rate: 200 rpm).

### 3.3. Adsorption isotherms

Several mathematical models have been applied in describing equilibrium studies for the removal of pollutants by adsorption on solid surfaces. Out of several isotherm equations, Freundlich, Langmuir, and Dubinin–Kaganer–Radushkevich isotherm equations have been reported most frequently. These equations were applied to the obtained effective conditions.

#### 3.3.1. Freundlich isotherm

The Freundlich adsorption isotherm (1906) based on the adsorption phenomenon occurred on heterogeneous surfaces. The isotherm assumes that the surface sites of the adsorbent have a spectrum of different binding energies.

It has the following form:

$$q_e = k_F C_e^{\ 1}/n \tag{3}$$

Eq. (3) can be expressed in a linear form:

$$\log q_e = \log k_F + 1/n \log C_e \tag{4}$$

where $q_e$ is the equilibrium adsorption capacity, (mg/g) and $C_e$ is the equilibrium concentration of Cr (VI) in the solution (mg/L). $k_F$ represents the adsorption capacity when metal ion equilibrium concentration equals to 1 (mg/g), $n$ is the degree of dependence of adsorption with equilibrium concentration, and $k_F$ and $1/n$ are related to the adsorbent capacity and sorption intensity of the adsorbent, respectively.

The equilibrium data for Cr (VI) over the concentration range from 100 to 400 mg/L have been correlated with the Freundlich isotherm. A linear plot is obtained when log $C_e$ is plotted against log $q$ over the entire concentration range of Cr (VI) (Fig. 6). Values of $k_F$ and $1/n$ can be calculated from the intercept and the slope of this straight line, respectively.

The values of Freundlich constants, $k_F$ and $1/n$, obtained are shown in Table 1. The high $R_2$ values obtained are shown in the table. The value of $k_F$ calculated from the Freundlich model is large, which indicates that magnetite nanoparticles have a high adsorption affinity toward Cr (VI).

The Freundlich constant $(1/n)$ is related to the sorption intensity of the sorbent. When, $0.1 < 1/n \leqslant 0.5$, it is easy to adsorb; $0.5 < 1/n \leqslant 1$, there is some difficulty with the absorption; $1/n > 1$, there is a quite difficult with the absorption as stated by Treybal [26].

The $1/n$ value in the study was 0.348 (Table 1), which suggests that the adsorption process is favorable, then the adsorption capacity increases and new adsorption sites are formed [27].

#### 3.3.2. The Langmuir isotherm

The Langmuir adsorption isotherm was reported in 1918 and used to describe the adsorption phenomenon at the interface between solid and liquid phases for monomolecular layer. The Langmuir model assumes that the surface of the adsorbent is homogeneous, adsorption energy is uniform for each adsorption site, and solute uptake occurs by monolayer adsorption.

It can be represented in the linear form by the following equation:

$$\frac{C_e}{q} = \frac{1}{bq_{max}} + \frac{C_e}{q_{max}} \tag{5}$$

$q$ is the amount of metal ions sorbed per unit mass onto magnetite (mg/g), $q_{max}$ is maximum adsorption capacity at complete monolayer coverage (mg/g), and $b$ is a Langmuir constant that relates to the heat of adsorption (L/mg).

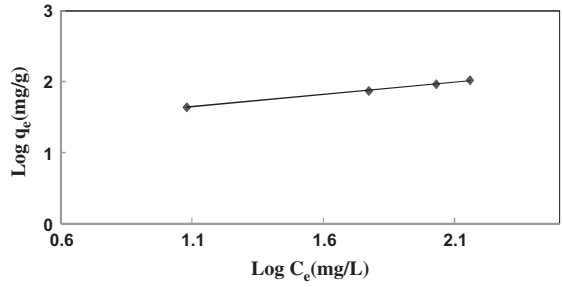


Fig. 6. The Freundlich isotherm plot for Cr (VI) adsorption by magnetite nanoparticles (pH: 5.5, contact time: 60 min, shaking rate: 200 rpm, and amount of adsorbent: 2 g/L).

Table 1
Freundlich, Langmuir, and DKR isothermal adsorption equation parameters for the adsorption of Cr (VI) by prepared magnetite nanoparticles (absorbent dose: 2 g/L, pH value: 5.5, initial concentration: 100–400 mg/L, contact time: 60 min, and agitation speed: 200 rpm)

| | | | | |
|---|---|---|---|---|
| Freundlich isotherm parameters | $1/n$ | $K_F$ (mg/g) | $R^2$ | |
| | 0.353 | 18.36 | 0.9986 | |
| Langmuir isotherm parameters | $q_{max}$ (mg/g) | $b$ (L/mg) | $R^2$ | |
| | 121.9 | 0.0355 | 0.9817 | |
| DKR isotherm parameters | $q_{max}$ (mol/g) | $\beta$ (mol$^2$/J$^2$) | $E$ (kJ/mol) | $R^2$ |
| | $3.87 \times 10^{-3}$ | $-0.360 \times 10^{-8}$ | 11.78 | 0.9808 |

A plot of $C_e/q_e$ vs. $C_e$ over the entire concentration range of metal ion investigated (Fig. 7). The values of $q_{max}$ and $b$ were determined by the slope and intercept of Fig. 7, and are given in Table 1. It was noted that the correlation coefficient ($R^2$) for Langmuir indicated a significant correlation. The results showed that the isothermal data better conformed to Freundlich equation.

### 3.3.3. Dubinin–Kaganer–Radushkevich isotherm (DKR isotherm)

The DKR isotherm is a semiempirical equation where adsorption follows a pore-filling mechanism. It assumes that the adsorption has a multilayer character, involves van der Waals forces, and is applicable for physical adsorption processes [28].

The sorption data were applied to the DKR model in order to distinguish between physical and chemical adsorption.

The linear form of the DKR model is:

$$\ln q = \ln q_{max} - \beta\varepsilon^2 \quad (6)$$

$\beta$ is the activity coefficient related to mean sorption energy (mol$^2$/kJ$^2$) and $\varepsilon$ is the Polanyi potential, which is equal to:

$$\varepsilon = RT\ln\left(1+\frac{1}{C_e}\right) \quad (7)$$

where $R$ is the ideal gas constant (8.3145 J /mol K), $\boldsymbol{T}$ is the absolute temperature ($K$).

The slope of the plot of ln $q$ vs. $\varepsilon^2$ gives $\beta$ (mol$^2$/J$^2$) and the intercept yields the maximum sorption capacity, $q_{max}$ (mol/g).

$E$ is defined as the free energy change (kJ/mol), which required transferring 1 mol of ions from solution to the solid surfaces. The relation is as follows:

$$E = \frac{1}{\sqrt{-2\beta}} \quad (8)$$

The plot of ln $q$ against $\varepsilon^2$ for Cr (VI) adsorption on magnetite nanoparticles is shown in Fig. 8 and DKR parameters are listed in Table 1.

The magnitude of $E$ is useful for estimating the mechanism of the adsorption reaction. Adsorption is dominated by chemical ion-exchange if $E$ is in the range of 8–16 kJ/mol, whereas physical forces may affect the adsorption in the case of $E < 8$ kJ/mol [29]. The $E$ value obtained from Eq. (9) is (11.78 kJ/mol), which is in the adsorption energy range of chemical ion exchange reactions. This suggests that Cr

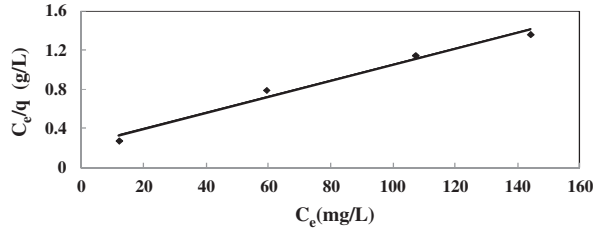


Fig. 7. The Langmuir isotherm plot for Cr (VI) adsorption by magnetite nanoparticles (pH: 5.5, contact time: 60 min, shaking rate: 200 rpm, and amount of adsorbent: 2 g/L).

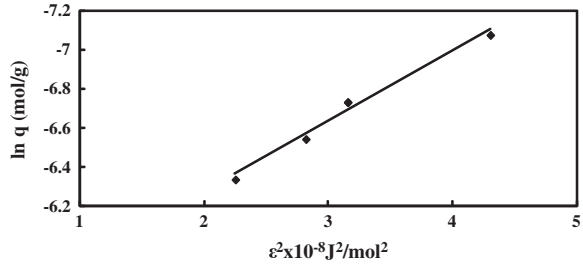


Fig. 8. The DKR isotherm plot for Cr (VI) adsorption by magnetite nanoparticles (pH: 5.5, contact time: 60 min, shaking rate: 200 rpm, and amount of adsorbent: 2 g/L).

(VI) adsorption onto magnetite nanoparticles is attributed to chemical adsorption rather than physical adsorption.

### 3.4. Adsorption kinetics

#### 3.4.1. Pseudo-first-order kinetics

The pseudo-first-order equation (Lagergren's equation) describes adsorption in solid–liquid systems based on the sorption capacity of solids. It is assumed that one chromium ion is sorbed onto one sorption site on the nanomagnetite surface [30].

The linear form of pseudo-first-order model can be expressed as:

$$\log(q_e - q_t) = \log q_e - \frac{k_1 t}{2.303} \quad (9)$$

where $q_e$ and $q_t$ are the amounts of adsorbed Cr (VI) on the adsorbent at equilibrium and at time $t$, respectively (mg/g), and $k_1$ is the first-order adsorption rate constant ($min^{-1}$).

The linearized form of the pseudo-first-order model for the sorption of Cr (VI) ions onto magnetite nanoparticles is given in Fig. 9 for initial concentration 20 mg/L. The calculated results of the first-order rate equation are given in Table 2. The $q_e$ value acquired by this method is contrasted with the experimental value. So, the reaction cannot be classified as first order.

#### 3.4.2. Pseudo-second-order kinetics

In order to find a more reliable description of the kinetics, second-order kinetic equation was applied. The pseudo-second-order kinetics can be represented by the following linear equation [31]:

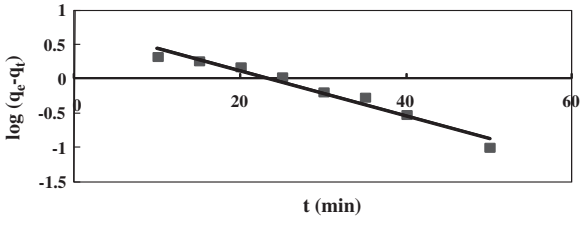


Fig. 9. Pseudo-first-order sorption kinetics of Cr(VI) onto magnetite nanoparticles (absorbent dose: 2 g/L, pH value: 5.5, initial concentration: 20 mg/L, contact time: 10, 15, 20, 25, 30, 35, 40, 50, and 60 min, and agitation speed: 200 rpm).

$$\frac{T}{q_t} = \frac{1}{k_2 q_e^2} + \frac{1}{q_e} t \quad (10)$$

where $k_2$ is the pseudo-second-order rate constant of adsorption (gm/g min).

Linear plot of $t/q_t$ vs. $t$ is achieved according to Eq. (11) (Fig. 10). The $k$ and $q_e$ values calculated from the slope and intercept are summarized in Table 2.

The correlation coefficients of the pseudo-second-order equation for the linear plots are very close to 1. Besides, the calculated $q_e$ values agreed very well with the experimental data. These experimental results support the assumption behind the model that the rate-limiting step in adsorption is chemisorption involving valence forces through the sharing or exchange of electrons between adsorbent and metal ions.

#### 3.4.3. Elovich kinetic model

The Elovich kinetic model [32] is based on chemisorption phenomena and is expressed as:

$$\frac{dq}{dt} = \alpha \exp(-\beta q_t) \quad (11)$$

To simplify the Elovich equation, Chien and Clayton [33] assumed $\alpha\beta t >> t$ and by applying boundary conditions $q_t = 0 =$ at $t = 0$ and $q_t = q_t$ and $t = t$, Eq. (12) yields Eq. (13), where $\alpha$ (mg/g min) is the initial sorption rate and the parameter $\beta$ (g/mg) is related to the extent of surface coverage and activation energy for chemisorption. The kinetic results will be linear on a $q_t$ vs. ln ($t$) plot (Fig. 11) and the constants $\alpha$ and $\beta$ can be computed from the slope and intercept of the graph.

Table 2 lists the kinetic constants obtained from the Elovich equation. The correlation coefficients are lower than those of the pseudo-second-order equation.

#### 3.4.4. Intraparticle diffusion model

The Weber's diffusion model [34] is the most commonly used technique for identifying the mechanism involved in the adsorption process.

The adsorption process may be controlled by: (1) Film diffusion, where the adsorbate transports to the external surface of the adsorbent. (2) Particle diffusion, where the adsorbate transports within the pores of the adsorbent except for a small amount of adsorption that occurs on the external surface. (3) Surface diffusion adsorption, where the adsorption occurs on the exterior surface of the adsorbent.

Table 2
Kinetic parameters for Cr (VI) adsorption by prepared magnetite nanopartics (absorbent dose: 2 g/L, pH value: 5.5, initial concentration: 20 mg/L, contact time: 10–120 min, and agitation speed: 200 rpm)

| | | | | |
|---|---|---|---|---|
| Pseudo-first-order | $q_e$ (mg/g) (calculated) | $q_e$ (mg/g) (experiment) | $K_1$ ($min^{-1}$) | $R^2$ |
| | 5.9 | 9.6 | 0.07 | 0.9621 |
| Pseudo-second-order | $q_e$ (mg/g) (calculated) | $q_e$ (mg/g) (experiment) | $K_2$ (g/mg min) | $R^2$ |
| | 9.9 | 9.6 | 0.028 | 0.9994 |
| *Elovich kinetic model* | $\alpha$ (mg/g min) | | $\beta$ (g/mg) | $R^2$ |
| | 94.9 | | 0.91 | 0.9351 |

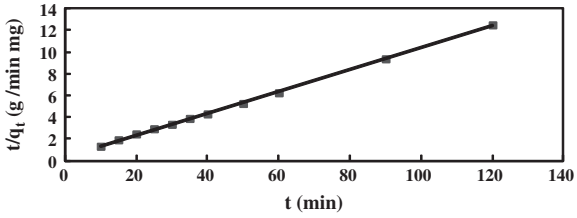


Fig. 10. Pseudo-second-order sorption kinetics of Cr (VI) onto magnetite nanoparticles (absorbent dose: 2 g/L, pH value: 5.5, initial concentration: 20 mg/L, contact time: 10, 15, 20, 25, 30, 35, 40, 50, 60, 90, and 120 min, and agitation speed: 200 rpm).

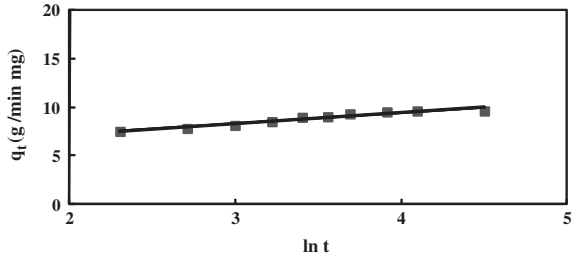


Fig. 11. Elovich sorption model for Cr (VI) adsorption onto magnetite nanoparticles (absorbent dose: 2 g/L, pH value: 5.5, initial concentration: 20 mg/L, contact time: 10, 15, 20, 25, 30, 35, 40, 50, 60, and 90 min, and agitation speed: 200 rpm).

Usually, external transport is the rate-limiting step in systems, which have poor mixing; dilute concentration of adsorbate; and small particle size.

The Weber's diffusion model is expressed as:

$$q_t = k_d t^{1/2} + C \tag{12}$$

Plots of $q_t$ vs. $t^{1/2}$ for the initial concentration can achieve the value of intraparticle diffusion rate constant $K_d$ (mg/g $min^{1/2}$) (Fig. 12), the intercept $C$ is a constant (mg/g) which gives an idea about the thickness of the boundary layer on the adsorbent surface.

If a straight line passing through the point of origin is obtained, therefore, sorption of Cr (VI) on magnetite nanoparticles followed intraparticle diffusion mechanism only.

Fig. 12 indicates that the plot of $q_t$ vs. $t^{1/2}$ is linear before reaching equilibrium state and the line is not passing through the origin, implying that more than one process affected the sorption of Cr (VI) and the intraparticle diffusion is not the rate-limiting step for the whole reaction. The values of model parameters calculated from the slopes of the linear plots obtained are given in Table 2.

In order to determine the actual rate-controlling step involved in the sorption process, the kinetic data have been analyzed using the model given by Boyd et al. [36].

$$B = \frac{D_i \pi^2}{r^2} \tag{13}$$

where $B$ is the time constant ($min^{-1}$), $D_i$ is the effective diffusion coefficient of the metal ions in the sorbent phase ($cm^2$/min), $r$ is the radius of the sorbent particle (cm) assumed to be spherical, and m is an integer that defines the infinite series solution. Bt is given by the equation:

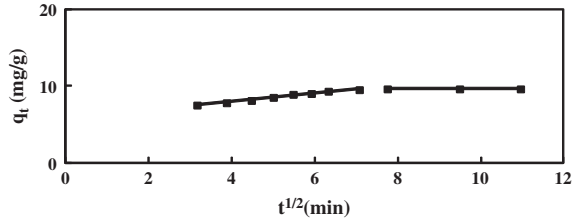


Fig. 12. Intraparticle diffusion plots for for Cr (VI) adsorption onto magnetite nanoparticles (absorbent dose: 2 g/L, pH value: 5.5, initial concentration: 20 mg/L, contact time: 10, 15, 20, 25, 30, 35, 40, 50, 60, 90, and 120 min, and agitation speed: 200 rpm).

$$Bt = -0.49770 - \ln(1 - F) \quad (14)$$

The calculated *Bt* values were then plotted against time. A straight line passing through the origin indicates that the process was governed by particle diffusion mechanisms otherwise they are governed by film diffusion [36]. The results show that the plots are linear in the initial period of sorption and do not pass through the origin. This indicates that the adsorption kinetics is not limited to only pore diffusion or, in other words, the diffusion of the adsorbate into the pores of the adsorbents is not the only rate-controlling step.

### 3.5. Desorption of Cr (VI) and reusability of nanomagnetite

The primary objective of desorption is to restore the adsorption capacity of the exhausted adsorbent, while the secondary objective is to recover valuable components present in the adsorbed phase, if any.

Ten milli litre of 1 and 5 M from each eluant were mixed with Cr-adsorbed magnetite for 2 h. The desorption efficiencies of $HNO_3$ and HCl were found to be 90 and 65% at 1 M concentration, respectively. The desorption efficiency increased at 5 M concentration of $HNO_3$ and HCl solution to reach 94 and 75%, respectively.

To study the reusability of nanoadsorbent, experiments pertaining to magnetite regeneration and Cr (VI) readsorption were carried out in five consecutive cycles. For each cycle, 10 mL of 100 mg/L Cr (VI) solution was adsorbed by 20 mg magnetite nanoparticles for 1 h and then desorbed with 10 mL of 5 M $HNO_3$ and stirring for 2 h. After each cycle of adsorption–desorption, the adsorbent was washed thoroughly with distilled water to neutrality, then dried, and reconditioned for adsorption in the succeeding cycle. The results show that the efficiencies of the recycled sorbent for removing Cr (VI) are nearly the same as those for the fresh one even after three times recycling.

## 4. Conclusions

The efficiency of magnetite nanoparticles for removing Cr (VI) ions from aqueous solutions has been investigated. Adsorption was very rapid and equilibrium was achieved in 1 h. Also, adsorption was highly dependent on the initial concentration of Cr (VI), pH, and adsorbent dose. Maximum removal was observed at pH between 5 and 6.

Adsorption increased as the initial concentration of Cr (VI) decreased.

The adsorption data were well fitted by both the Langmuir and Freundlich isotherms and the pseudo-second-order kinetics. The regeneration studies also showed that magnetite nanoparticles can be used several times for the sorption of Cr (VI) from aqueous solutions without loss of their magnetic properties.

Therefore, magnetite nanoparticles are considered as fast, effective, and inexpensive adsorbents for rapid removal and recovery of metal ions and could be used as an alternate to conventional adsorbents for the removal of metal ions from wastewater.

## References

[1] S.H. Jang, G.Y. Jeong, B.G. Min, W.S. Lyoo, S.C. Lee, Preparation and lead ion removal property of hydroxyapatite/polyacrylamide composite hydrogels, J. Hazard. Mater. 159 (2008) 294–299.
[2] L. Zhou, Y. Wang, Z. Liu, Q. Huang, Characteristics of equilibrium, kinetics studies for adsorption of Hg (II), Cu(II), and Ni(II) ions by thiourea-modified magnetic chitosan microspheres, J. Hazard. Mater. 161 (2009) 995–1002.
[3] F. Iemma, G. Crillo, U.G. Sipizzirri, F. Puoci, O.I. Parisi, N. Picci, Removal of metal ions from aqueous solution by chelating polymeric microspheres bearing phytic acid derivatives, Eur. Polym. J. 44 (2008) 1183–1190.
[4] S. Pramanik, S. Dey, P. Chattopadhyay, A new chelating resin containing azophenolcarboxylate functionality: Synthesis, characterization and application to chromium speciation in wastewater, Anal. Chim. Acta 584 (2007) 469–476.
[5] E.A. Ayuso, A.G. Sanchez, X. Querol, Purification of metal electroplating waste waters using zeolites, Water Res. 37 (2003) 4855–4862.
[6] EPA (Environmental Protection Agency). Drinking Water Contaminants, Environmental Protection Agency, Washington, DC, 2010.
[7] B.L. Finley, B.D. Kerger, M.W. Katona, M.L. Gargas, G.C. Corbett, D.J. Paustenbach, Human ingestion of chromium (VI) in drinking water: Pharmacokinetics following repeated exposure, Toxicol. Appl. Pharmacol. J. 142 (1997) 151–159.
[8] EPA Toxicological Review of Hexavalent Chromium (CAS No. 18540-29-9) (External Review Draft) 2010, EPA/635/R-10/004A.
[9] OEHHA (Office of Environmental Health Hazard Assessment), Draft Public Health Goal for Hexavalent Chromium in Drinking Water: Pesticide and Environmental Toxicology Branch. Office of Environmental Health Hazard Assessment, California Environmental Protection Agency, 2009.
[10] A. Özcan, A.S. Özcan, S. Tunali, T. Akar; I. Kiran, Determination of the equilibrium, kinetic and thermodynamic parameters of adsorption of copper (II) ions onto seeds of Capsicum annuum, J. Hazard. Mater. 124 (2005) 200–208.
[11] A. Mellah, S. Chegrouche, M. Barkat, The removal of uranium (VI) from aqueous solutions onto activated carbon: Kinetic and thermodynamic investigations, J. Colloid Interf. Sci. 296 (2006) 434–441.
[12] A.K. Meena, G.K. Mishra, P.K. Rai, C. Rajagopal, P.N. Nagar, Removal of heavy metal ions from aqueous solutions using carbon aerogel as an adsorbent, J. Hazard. Mater. 122 (2005) 161–170.
[13] P.C. Manuel, M.M. Jose, T.M. Rosa, Chromium (VI) removal with activated carbons, Water Res. 29 (1995) 2174–2180.
[14] N.R. Bishnoi, M. Bajaj, N. Sharma, A. Gupta, Adsorption of Cr (VI) on activated rice husk carbon and activated alumina, Bioresour. Technol. 91 (2004) 305–307.

[15] D. Gang, S. Hu, K. Banerji, T.E. Clevenger, Modified poly-(4-vinylpyridine) coated silica gel. Fast kinetics of diffusion-controlled sorption of chromium (VI), Ind. Eng. Chem. Res. 40 (2001) 1200–1204.
[16] V.K. Garg, R.K. Gupta, Adsorption of chromium from aqueous solution on treated sawdust, Bioresour. Technol. 92 (2004) 79–81.
[17] J. Hu, G.H. Chen, I.M.C. Lo, Selective removal of heavy metals from industrial wastewater using maghemite nanoparticle: Performance and mechanisms, J. Environ. Eng. 132 (2006) 709–715.
[18] M. Ozmen, K. Can, G. Arslan, A. Tor, Y. Cengeloglu, M. Ersoz, Adsorption of Cu (II) from aqueous solution by using modified $Fe_3O_4$ magnetic nanoparticles, Desalination 254 (2010) 162–169.
[19] R.M. Cornell, U. Schertmann, Iron Oxides in the Laboratory; Preparation and Characterization. Weinheim, VCH, 1991.
[20] A.K. Gupta, M. Gupta, Synthesis and surface engineering of iron oxide nanoparticles for biomedical applications, Biomaterials 26 (2005) 3995–4021.
[21] Y.C. Sharma, V. Srivastava, C.H. Weng, S.N. Upadhyay, Removal of Cr (VI) from wastewater by adsorption on iron nanoparticles, Can. J. Chem. Eng. 87 (2009) 921–929.
[22] APHA, Standard Methods for the Examination of Water and Wastewater, 21st ed., American Public Health Association, Washington, DC, 2005.
[23] A. Smara, R. Delimi, E. Chainet, J Sandeaux, Removal of heavy metals from diluted mixtures by a hybrid ion-exchange/electro dialysis process, Sep. Purif. Technol. 57 (2007) 103–110.
[24] K. Kim, E. Kim, J. Lee, S. Maeng, Y. Kim, Synthesis and characterization of magnetite nanopowders, Curr. Appl. Physi. 8 (2008) 758–760.
[25] J. Hu, I.M.C. Lo, G. Chen, Removal of Cr (VI) by magnetite nanoparticle, Water Sci. Technol. 50 (2004) 139–146.
[26] R.E. Treybal, Mass-Transfer Operations, 3rd ed., McGraw-Hill international, Singapore, 1981.
[27] A.S. Ozcan, B. Erdem, A. Ozcan, Adsorption of Acid Blue 193 from aqueous solutions onto Na–bentonite and DTMA–bentonite, J. Colloid Interf. Sci. 280 (2004) 44–54.
[28] G.E. Boyd, A.W. Adamson, L.S. Myers, The exchange adsorption of ions from aqueous solutions on organic zeolites, J. Am. Chem. Soc. 69 (1947) 2836–2848.
[29] N.D. Hutson, R.T. Yang, Theoretical basis for the Dubinin–Radushkevitch (D–R) adsorption isotherm equation, Adsorption 3 (1997) 189–195.
[30] Y.-M. Hao, M. Chen, Z.-B. Hu, Effective removal of Cu (II) ions from aqueous solution by amino-functionalized magnetic nanoparticles, J. Hazard. Mater. 184 (2010) 392–399.
[31] Y.S. Ho, Citation review of Lagergren kinetic rate equation on adsorption reactions, Scientometrics 59 (2004) 171–177.
[32] Y.S. Ho, Review of second-order models for adsorption systems, J. Hazard. Mater. 136 (2006) 681–689.
[33] D.L. Sparks, Kinetics of reaction in pure and mixed systems in Soil Physical Chemistry, CRC Press, Boca Raton, FL, 1986, pp. 12–18.
[34] S.H. Chien, W.R. Clayton, Application of elovich equation to the kinetics of phosphate release and sorption on soils, Soil Sci. Soc. Am. J. 44 (1980) 265–268.
[35] W.J. Weber, J.C. Morris, Kinetics of adsorption on carbon from solutions, J. Environ. Eng. Div. 89 (1963) 31–60.
[36] X. Hu, J. Wang, Y. Liu, X. Li, G. Zeng, Z. Bao, X. Zeng, A. Chen, F. Long, Adsorption of chromium (VI) by ethylenediamine-modified cross-linked magnetic chitosan resin: Isotherms, kinetics and thermodynamics, J. Hazard. Mater. 185 (2011) 306–314.